LEGIBILITY NOTICE

A major purpose of the Technical Information Center is to provide the broadest dissemination possible of information contained in DOE's Research and Development Reports to business, industry, the academic community, and federal, state and local governments.

Although a small portion of this report is not reproducible, it is being made available to expedite the availability of information on the research discussed herein.

LA-UR-88-1167

CONF-880844--3

Los Alamos National Laboratory is operated by the University of California for the United States Department of Energy under contract W-7405-ENG 36

LA-UR--88-1167

DE88 009156

TITLE METASTABLE ALLOY PHASES PREPARED BY SOLID STATE REACTIONS AND BALL MILLING

AUTHOR(S) R. B. Schwarz, CMS

SUBMITTED TO Talk to be given at the 8th International Conference on the Strength of Metals and Alloys (ICSMA) at Tampere, Finland on August 22-26, 1988. To be published by Pergamon Press. (INVITED PAPER)

DISCLAIMER

Los Alamos National Laboratory
Los Alamos, New Mexico 87545

METASTABLE ALLOY PHASES PREPARED BY SOLID STATE REACTIONS AND BALL MILLING

R. B. Schwarz

Center for Materials Science
Los Alamos National Laboratory
Los Alamos, NM 87545, USA.

ABSTRACT

The main methods of synthesis of amorphous metallic alloys are based on (a) the rapid solidification of alloys from the liquid or vapor phase, (b) solid state interdiffusion reactions between pure metals having negative heats of mixing, and (c) mechanical attrition of a crystalline intermetallics. The first method received a major impetus in 1960 with the experiments of Pol Duwez and co-workers. We describe methods (b) and (c), developed around 1983, and we discuss recent advances in the understanding of the glass forming ranges for the three methods of synthesis.

KEYWORDS

Amorphous alloys; glassy alloys; solid state reactions; mechanical alloying; mechanical grinding; glass forming range

INTRODUCTION

Metastable non-crystalline solid phases can be produced by a variety of techniques, including (a) solidification from the liquid or vapor phases, (b) solid state reactions between pure elements, (c) mechanical deformation of crystalline lattices, (d) deposition from a chemical solution, and (e) high-energy ion-, electron-, or neutron bombardment of crystalline materials.

Non-crystalline solids formed by continuous cooling from the liquid state are commonly known as glasses. Ionic and covalent glasses often form when the corresponding melt fails to crystallize during relatively slow cooling. In these, the directional nature of the inter-atomic bonds limits the rate at which the atoms or molecules can rearrange to maintain thermodynamic equilibrium during cooling, and thus the melt solidifies into a glass even at cooling rates as low as 10^{-2} K s^{-1}. Metallic melts, in contrast, have non-directional bonding, and thus exhibit far less resistance to crystallize and do not form glasses unless cooled at much higher rates. Buckel and Hilsch (1954) demonstrated that amorphous thin films of pure metals could be formed by condensing the metal vapor onto a cryogenically cooled substrate,

a process that gives an equivalent cooling rate of the order of 10^{12} K s^{-1}. In these films the amorphous phase was most likely stabilized by impurities. The removal of the impurities lowers the crystallization temperature, T_x, and in some cases prevents the formation of amorphous films of pure metals even for substrates kept at 4 °K. The field of amorphous alloys grew at a fast rate following the experiments of Pol Duwez and co-workers (1960) who developed a variety of techniques to rapidly solidify alloy melts at cooling rates of 10^6 to 10^8 K s^{-1}. It soon became apparent that the glass forming range (GFR) of metallic alloys is strongly composition dependent, being easier to form metallic glasses near the compositions of *deep* eutectics in the phase diagram. At these compositions the temperature interval between the liquidus, T_ℓ, and the glass transition temperature, T_g, is reduced so that the probability of being able to cool the melt through the interval without inducing crystallization is enhanced. Thus, there is a tendency for the GFR to vary inversely with the reduced glass transition temperature, $T_{rg} = T_g/T_\ell$. For alloys with low T_{rg}, the required cooling rates to avoid crystallization are large and thus one dimension of the amorphous product must be small (50 μm or less for cooling rates of the order of 10^6 K s^{-1}). For alloys with large T_{rg}, such as $Pd_{40}Ni_{40}P_{20}$ ($T_{rg} \approx 0.67$), the cooling rate requirement is relaxed allowing the preparation of cm-size amorphous samples at cooling rates of few K s^{-1} (Drehman, Greer, and Turnbull, 1982).

New methods of synthesis of amorphous metallic alloys have been developed over the last 10 years that are based on solid state reactions and on mechanical deformation. Contrary to the rapid solidification technique, the newer methods are performed at a constant temperature that is lower than the crystallization temperature of the amorphous alloy to be formed. Malik and Wallace (1977) and Yeh, Samwer and Johnson (1983) showed that the reaction of certain crystalline intermetallics with hydrogen leads to the formation on an amorphous hydride. In 1983, Schwarz and Johnson demonstrated that amorphous La-Au alloy films can be formed by a low thermal anneal of crystalline thin films of pure lantharum and gold. White (1979) and Koch and co-workers (1983) demonstrated that amorphous alloy powders can be prepared by mechanically alloying a mixture of powders of two pure metals. In the following sections we describe the synthesis of amorphous thin films by inter diffusion reactions and the synthesis of amorphous metallic powders by mechanical alloying. Various other aspects of the crystal to glass transformations in metallic materials have been reviewed by Johnson (1986).

AMORPHOUS THIN FILMS PREPARED BY SOLID-STATE REACTIONS

The solid state amorphizing reaction (SSAR) method requires clean (oxide free) interfaces between two reacting metals. Such interfaces can be obtained by depositing crystalline thin films of metals A and B in a high vacuum. Typically, films of a few tenths of a nm in thickness can be fully reacted within a few hours. Stacks of alternating thin films, as shown in Fig. 1, allow for the synthesis of thick amorphous layers. The chosen reaction temperature, T_r, is a few tens to a few hundred Kelvin lower than T_x. Three requirements have been proposed for the SSAR (Schwarz and Johnson, 1983; Schwarz, 1986): (1) metals A and B must have a large negative heat of mixing in the amorphous phase, (2) metals A and B must have vastly different diffusivities in each other and in the amorphous alloy to be formed, and (3) the binary system AB should have no stable crystalline phase in which the sub-lattice of the larger atom can be derived by a diffusionless transformation from the crystalline lattice of the larger atom. The first condition ensures that a thermodynamic driving force for the reaction exists. The negative heat of mixing also favors the reaction

kinetics by increasing the chemical diffusivities (Darken, 1948). The second condition ensures that the SSAR will be kinetically favored over the formation of crystalline intermetallic compounds. This favoring occurs because one species diffusing in the other and in the amorphous alloy is sufficient for the SSAR; generally, the formation of intermetallics, which have crystalline structures quite different from those of the two starting metals, requires the atomic motion of both species. Thus, a *temperature window* opens for the SSAR by choosing a pair of elements with vastly different diffusivities from each other while in the amorphous phase. The third condition ensures that the binary system does not have a crystalline intermetallic that can be formed when the smaller atom diffuses through the crystalline lattice of the larger one, i.e., by the same mechanism responsible for the SSAR. If this mechanism was possible, the interdiffusion reaction could lead to forming stable crystalline intermetallics that have a free energy lower than that of the metastable amorphous alloy.

Figure 2 illustrates the *temperature window* for the SSAR, showing the electrical resistance, R, of a stack of alternating thin films of Ni and Zr during the continuous heating from 300 to 1000 K, followed by a cooling to 300 K (Rubin and Schwarz, 1988). The labels (a), (b) and (c) in this figure correspond to those in Fig. 1. From (a) to (b), the films do not interdiffuse and R increases linearly with increasing temperature, which is expected for pure crystalline metals. At the temperature of (b), an amorphous alloy begins to form at the Ni/Zr interfaces (see also Fig. 1). Because the resistivity of the amorphous alloy is larger than that of the pure Ni and Zr used to form the alloy, the resistance of the multilayer film increases. The SSAR ends at (c), when all the Ni and Zr have been consumed (see Fig. 1). From (c) to (d) the resistance is temperature independent and agrees with the usual observation that the resistivity of amorphous alloys is largely temperature independent. At (d) the amorphous alloy formed by SSAR begins to crystallize and the resistance decreases because the crystalline order introduced in the alloy allows for an easier electronic conduction. At point (e) the alloy has reached a thermodynamically stable state that is impervious to further temperature variations. The resistance of the crystalline alloy has a positive linear temperature dependence, as expected. The *temperature window* for the SSAR is clearly that between points (b) and (d). In the present understanding of the SSAR, point (b) denotes the onset of Ni diffusion (the smaller atom) in the amorphous alloy, while point (d) denotes the onset of Zr diffusion (the larger atom) in the amorphous alloy.

The SSAR has been observed in a large number of thin film couples. Some are: Au-La, Au-Ti, Au-Y, Au-Zr, Co-Sn, Co-Zr, Cr-Ti, Fe-Zr, Ni-Ti, and Ni-Zr. These systems clearly satisfy the first two requirements for the SSAR listed above - they all have a large negative heat of mixing (Niessen and co-workers, 1976) and the first element in each pair is an anomalously fast diffuser in the crystalline lattice of the second element (Le Claire, 1978). The requirement that the two elements have vastly different diffusivities in the amorphous alloy has only been tested for the Ni-Zr system (Cheng, Nicolet, and Johnson, 1985; Hahn, Averback and Rothman, 1986), where the diffusivity of Ni in amorphous NiZr alloy is some three orders of magnitude larger than that of Zr. Violations of the third condition for SSARs has been observed in the Nb-Sn system (Kim and Koch, 19xxx) and in the Ni-Sn system (Tiainen and Schwarz, 1988).

Figure 3 shows the products of an SSAR in multilayers of La and Au of different thickness ratios. The x-ray scattered intensities as a function

of scattering angle are for an unreacted (as deposited) sample (curve d) and for three samples with different average composition that were annealed *in situ* at 70 °C for the times shown in Fig. 3. Curve (a) is for a multilayer sample whose overall composition was La-rich; (b) is for a sample of near equi-atomic composition; and sample (c) is for a Au-rich sample (≃ 80 at. % Au). Pattern (d) shows the characteristic diffraction peaks of La and Au. The thermally reacted sample (b) has undergone a nearly complete transformation to an amorphous alloy. The La-rich and Au-rich samples, (a) and (c), have formed amorphous alloy coexisting with residual La and Au.

THERMODYNAMIC ASPECTS OF THE SOLID-STATE AMORPHIZING REACTION

Schwarz and Johnson (1983) showed that the products of SSARs and their homogeneity ranges are close to those predicted by a free-energy diagrams evaluated at the reaction temperature. In these diagrams the amorphous phase is treated as an undercooled liquid. Experience has shown that free-energy diagrams that predict the SSAR products quantitatively are difficult to construct. The difficulty arises in estimating the difference between the specific heats of the amorphous and crystalline alloy phases in the temperature regime between T_g and the melting temperature, T_m. Because this difference is not known, it is difficult to calculate the difference between the free energies of the amorphous and crystalline terminal solid solution phases at the reaction temperature T_r. The construction of free energy diagrams for specific binary systems are discussed by Schwarz and Johnson (1983), Schwarz, Petrich, and Saw (1985), Saunders and Miodownik (1986), Zöltzer and Bormann (1987), and Tiainen and Schwarz (1987). In the present discussion we will use a simplified free energy diagram.

Figure 4a is a schematic phase diagram for a binary system, A-B, that has a negative heat of mixing in the liquid phase. Phases α and β are crystalline primary solid solutions and phase γ is a crystalline intermetallic. Figure 4b shows the free energies of phases α, β, and γ and of the amorphous phase, λ, evaluated at T_r. Phase λ is treated as an undercooled liquid. If the interdiffusion reaction at the A/B interfaces in Fig. 1 reached a state of thermodynamic equilibrium, the reaction products would be determined by the common tangents between α, β, and γ in Fig. 4b (these tangents are not shown). However, if the reaction temperature is within the *temperature window*, insufficient thermal activation exists to promote the nucleation and growth of the crystalline phase γ. In the absence of phase γ, the SSAR products are determined by the common tangents between phases α, β, and λ (shown in Fig. 4b). These tangents predict five reaction products: a crystalline solid solution, α, for $0 < x < x_1$; a two-phase product of $\alpha(x_1)$ and $\lambda(x_2)$; a single-phase amorphous alloy, λ, for $x_2 < x < x_3$; a two-phase product of $\lambda(x_3)$ and $\beta(x_4)$; and the crystalline solid solution, β, for $x_4 < x < 1$. We note that the GFR for alloys prepared by SSARs is wide and continuous and is located near the center of the composition range. For the La-Au system and $T_r = 400$ K, $x_2 \approx 0.2$ and $x_3 \approx 0.65$ (Schwarz and Johnson, 1983).

The glass-forming ranges (GFR) for alloys prepared by SSARs and by the RS of melts are quite different. In contrast to the SSAR method, the GFR for the rapid solidification method at cooling rates of the order of 10^6 K s^{-1} is usually fragmented into several narrow regimes located between the composition of intermetallic compounds that melt congruently. This fragmentation happens because preventing a molten alloy from crystallizing partitionlessly during cooling (without the need for long-range diffusion) is difficult near the compositions of these intermetallics (Nash and Schwarz, 1987). Furthermore, the liquidus of binary alloys with large

negative heats of mixing is usually low (deep eutectics) at compositions between those of congruent-melting intermetallics. Because T_x depends weakly on alloy composition, T_{rg} is largest near the eutectic compositions and the avoidance of crystallization during the cooling of the liquid is then easier to achieve. The bands at the bottom of Fig. 4b predict the GFRs for the SSAR and the RS methods applied to our hypothetical binary system. For the SSAR method the GFR equals the regime (x_2, x_3) predicted by the common tangents in the free energy diagram in Fig. 4b. For the RS method the GFR consists of two regimes, (x_2',x_c') and (x_c'',x_3'). We have estimated these regimes qualitatively based on Figs. 4a and 4b and on the notion that the formation of metallic glass during the continuous cooling of the melt requires avoiding partitionless crystallization. Previous calculations (Nash and Schwarz, 1988) predict that the values of x_2', x_c', x_c'', and x_3' are determined by the intersections of the T′ curves for the three crystalline phases, α, β, and γ, and the T_g-versus composition curve. The T′ curves are the temperature-composition locus for the formation of a given volume fraction of crystallized material by partitionless crystallization during the cooling of the melt at a constant rate. Partitionless crystallization during the RS of melt is thermodynamically driven by the difference between the free energies of the undercooled liquid and crystalline phases. Because crystallization must overcome a nucleation barrier, for a finite cooling rate we must have $x_2' < x_{o\alpha}$, $x_c' > x_{o\gamma}$, $x_c'' < x_{o\gamma}$, and $x_3' > x_{o\beta}$. Notice that the compositions x_2' and x_3' lie *outside* the corresponding T_o-points for the terminal solid solutions, $x_{0\alpha}$ and $x_{0\beta}$, while the extreme compositions of the amorphous phase formed by the SSAR, x_2 and x_3, lie *inside* the T_o-points. Furthermore, with increasing cooling rates the amorphous composition ranges (x_2',x_c') and (x_c'',x_3') become wider and the gap (x_c',x_c'') may eventually close. In contrast to the results for the RS method, the amorphous-phase homogeneity range for the SSAR method, (x_2,x_3), is certainly independent of kinetics (provided the reaction is carried on to completion) and has a weak dependence on T_r (Zöltzer and Bormann, 1987).

AMORPHOUS ALLOY POWDERS PREPARED BY MECHANICAL ALLOYING

Amorphous metallic alloys in powder form can be produced by mechanical alloying (MA) (White 1979; Koch et al. 1983; Schwarz et al , 1985; Hellstern and Schultz, 1986). MA is a high-energy ball milling process that was developed for synthesizing dispersion-strengthened alloy powders (Benjamin and Volin, 1974; Benjamin, 1976). For the synthesis of amorphous alloy powders by MA, elemental crystalline powders are placed into a sealed, hardened-steel or tungsten carbide container together with balls of the same material. The strong agitation of the balls in the container repeatedly deforms, breaks, and cold welds the powder particles trapped between colliding balls.

To date, the majority of the amorphous powders that have been prepared by MA are binary alloys of the early-transition metals titanium and zirconium and various 3-d late-transition metals: Ti-(Mn, Fe, Co, Ni, Cu) and Zr-(Mn, Fe, Co, Ni, Cu). Other systems in which amorphous alloy powder was prepared by MA include Ti-Pd, Nb-Ni, Hf-Al, Sn-Ni and Ti-Pd-Cu. Amorphous powders containing metalloids, such as $Fe_{80}B_{20}$, have been found more difficult to prepare by MA. For the metal-metal systems, the powder morphology changes characteristically with increasing MA time. After a short MA time, most of the powder in the container adheres to the balls and to the contained walls, giving them and *orange-peel* appearance. For a mixture of nickel and titanium powders mechanically alloyed for 0.5 h, the free particles have the

flake morphology shown in Fig. 5 (Petrich, 1986). Figure 6 shows a SEM micrograph of the cross section of a flake-shape particle. The alternating dark and light bands correspond to nickel and titanium, respectively. We believe that the adherence of the powder to the walls of the container and to the balls, as well as the formation of a layered structure, is a consequence of the the large chemical affinity of titanium to nickel and iron. This affinity increases the probability the during the initial collisions the titanium particles will cold weld to the two late-transition metals. Following the coating of the balls and walls with titanium, there is a tendency for the next layer to be of nickel, and so on. The repeated collisions deforms the coatings and creates the layer structure. With increasing MA time, the average thickness of the layers decreases (Benjamin, 1976).

Once most of the alloy is amorphous, there is less tendency for the powder particles to stick to each other or to the balls and container walls. After a few hours of MA, the coatings on the balls and container walls break off and form a powder of spherical particles, as shown in Fig. 7. The cross-sectional SEM in Fig. 8 shows that the particles are now a single phase and x-ray diffraction reveals that this phase is amorphous. H. Kimura, M. Kimura and F. Takada (1988) used a high-energy rotating-arm attritor to mechanically alloy a mixture of cobalt and zirconium powders. The apparatus allowed the authors to monitor the temperature of the container and the torque applied to the rotating arm of the attritor. A plot of the torque versus MA time shows a sharp maximum after about 0.5 h of MA which the authors attribute to the ending of the SSAR at the Co-Zr interfaces. After 4 h of MA, there is an abrupt drop in both the torque and temperature which the authors attribute to the ending of the amorphization process and to an abrupt decrease in the average particle diameter. The signatures in the torque and temperature traces should correspond to the morphology changes shown in Figs. 5-8 but, unfortunately, the reported characteristic times cannot be compared with our measurements obtained using a differenc attritor.

Figure 9 shows x-ray diffraction patterns for a MA mixture of nickel and titanium powders in molar ratio 1:2 taken after the MA times indicated in the figure (Schwarz, Petrich and Saw, 1985). With increasing MA time, the integrated intensity of the Bragg peaks for the starting pure metals decreases and is replaced by the broad diffraction bands characteristic of the amorphous alloy phase.

As for the case of amorphous thin films prepared by SSARs, the reaction products from MA powder mixtures of an early- and a late-transition metal have been found in good agreement with the predictions from free-energy diagrams evaluated for the average ball-milling temperature. (See, for example, Fig. 1 in Schwarz, Petrich and Saw, 1985). This agreement has been considered supporting evidence to the claim that the amorphization process during MA involves a solid-state reaction similar to that observed in the thin film experiments. (Schwarz et al., 1985; Hellstern and Schultz, 1986). The chemical diffusion necessary for the SSAR at the metal-metal interfaces (see Fig. 6) is most likely assisted by the excess point and lattice defects generated by the severe plastic deformation of the particles and by the momentary temperature increase in the powder particles trapped between colliding balls. Although there are no direc measurements of this temperature increase, calculations (Schwarz, Petrich and Saw, 1985; Schwarz and Koch, 1985) suggest that the temperature increase is at most a few hundred Kelvin. These calculation rule out the possibility that the amorphous alloy results from the rapid solidification of melt pools formed

by the heterogeneous deposition of mechanical energy in the particles trapped between colliding balls.

For some binary alloy systems the GFR has been measured for both the RS and the MA synthesis methods. Fig. 10 (from Hellstern, Schultz and Eckert, 1988) shows the homogeneity ranges of amorphous alloys of zirconium and three late-transition metals prepared by RS and by MA. Although the equilibrium-phase diagrams of these alloys differs significantly from that in Fig. 4a, the measured GFRs show many of the features predicted by the simple free energy diagram in Fig. 4b. In the notation of Fig. 4b, Fig. 10 shows that for the three alloys $x_2' < x_2$ and $x_3' > x_3$, as predicted by Fig. 4b. In addition, the homogeneity range of the amorphous phase obtained by MA is continuous while that for the RS method is fragmented into zirconium-rich and zirconium-poor regimes.

Although the synthesis of amorphous powders by MA has been applied to a large variety of metal systems, less progress has been made in the consolidation of these powders into bulk amorphous products. Static techniques such as hot isostatic pressing are of limited value because it is difficult to hold the powder for long periods of time at a temperature close to T_g (in order to decrease the viscosity) while preventing its crystallization. Dynamic techniques such as shock-wave consolidation, which has been successfully applied to metastable *crystalline* alloy powders (Kasiraj and co-workers, 1984), is much more difficult to apply to amorphous powders because the amorphous compacts fracture easily during pressure release. Recently, Shingu (1988) has applied the strained-powder rolling method to obtain 100% dense amorphous $Fe_{78}B_{13}Si_9$ alloys. In this method the amorphous mechanically alloyed powder is placed inside a stainless-steel tube. Its ends are sealed and the tube is dipped into a molten salt bath kept at a temperature a few tens of Kelvin below T_x. After a short annealing time, the tube is removed from the bath and it is rolled hot. Densification and consolidation occurs because at temperatures close to T_x the amorphous alloy has a reduced viscosity.

ISOTHERMAL SYNTHESIS METHODS THAT DO NOT INVOLVE INTERDIFFUSION

The synthesis of amorphous alloys by SSAR and MA, discussed above, involves a chemical *reaction* and mass transport. The reaction occurs in response to a lowering of free energy in the system and involves the long-range diffusion of one of the species in the other and in the amorphous alloy phase previously formed. Several synthesis methods for amorphous alloys have been developed that are based on isothermal solid state transformations which do not involve composition changes. These methods include (a) the mechanical grinding of crystalline intermetallics, (b) massive transformations from a metastable crystalline phase to the amorphous phase (Von Allmen and Blatter, 1987), and (c) amorphization by irradiation with energetic particles such as electrons, neutrons, and ions. In the following we comment on method (a).

Yermakov, Yurchikov, and Barinov (1981, 1982) reported the formation of amorphous alloy powders of yttrium and cobalt by the mechanical grinding of crystalline intermetallics of these elements. The authors attributed the amorphization to the formation of melt near the particle surfaces, followed by the rapid solidification of this melt by heat conduction into the cooler regions of the particles. Schwarz and Koch (1985) showed that amorphous powders of $Ni_{33}Ti_{67}$ and $Ni_{45}Nb_{55}$ can be prepared by MA starting from a

mixture of elemental powders or by mechanically grinding (MG) crystalline powder of the intermetallics $NiTi_2$ and NiNb, respectively. Contrary to the previous work, these authors attributed the formation of the amorphous alloy by MG to the raising of the free energy of the intermetallic powder as a result of the accumulation of point and lattice defects and to the generation of chemical disorder.

Because in many alloy systems the amorphous powder can be produced by either MA or MG (Lee, Jang, and Koch, 1988), it is logical to ask whether during the MA of a mixture of powders of metals A and B, the amorphous alloy $(AB)_{am}$ forms by the direct reaction $A + B \rightarrow (AB)_{am}$ or through the indirect reaction $A + B \rightarrow (AB)_{cr} \rightarrow (AB)_{am}$, which involves the intermediate crystalline phase $(AB)_{cr}$. The literature has examples of both reactions. For example, in the MA of nickel and titanium powders to form amorphous $Ni_{1-x}Ti_x$ with $(0.3 < x < 0.7)$, Schwarz, Petrich and Saw (1985) found no evidence of the formation of intermetallic compounds at any stage of MA. On the other hand, Kim and Koch (19xxx) reported that during the MA of niobium and tin powders in molar ratio 3:1, a Nb_3Sn intermetallic (A15 structure) forms first which, with continued ball milling, transforms to an amorphous $Nb_{75}Sn_{25}$ alloy. An indirect amorphization reaction was also observed by Tiainen and Schwarz (1988) during the ball milling of nickel and tin, which we will discuss in more detail. In the composition range studied (0.2 to 0.4 molar percent tin), after 2 h of MA the powder was a mixture of crystalline α-nickel and Ni_3Sn_2. With increasing MA time, one of the crystalline phases was progressively consumed with the concurrent formation of amorphous $Ni_{75}Sn_{25}$. Which of the two crystalline phases was consumed depended on the average alloy composition: for $Ni_{1-x}Sn_x$ with $x < 0.25$, the crystalline Ni_3Sn_2 disappeared with increasing MA as it was replaced by amorphous $Ni_{75}Sn_{25}$. For $x > 0.25$, α-Ni was consumed as the amorphous $Ni_{75}Sn_{25}$ formed. For an initial mixture of nickel and tin powders with average composition $Ni_{75}Sn_{25}$, both crystalline compounds were consumed simultaneously during MA leading to the formation of amorphous $Ni_{75}Sn_{25}$. The authors notice that the *substructure* of tin in Ni_3Sn_2 can be derived from a diffusionless transformation applied to the lattice of pure tin (see Fig. 8 in Tiainen and Schwarz, 1988), and thus the nickel-tin system violates the third condition for the synthesis of amorphous alloys by SSAR, discussed earlier. The authors propose that the easy formation of Ni_3Sn_{2z} during the early stages of MA results from the diffusion of nickel into pure tin, without the need for the long-range diffusion of tin, i.e., by the same mechanism that operates during SSARs.

REFERENCES

Benjamin, J. S. (1976). Mechanical Alloying. *Sci. Am.* 234, 40-8.

Benjamin, J. S. and T. E. Volin (1974). The mechanism of mechanical alloying. *Metall. Trans.* 5, 1929-34.

Buckel, W. and R. Hilsch (1954). xxx. *Z. Phys.* 138, 109-xxx.

Cheng, Y. T., W. L. Johnson, and M-A. Nicolet, (1985). Dominant moving species in the formation of amorphous NiZr by solid state reaction. *Appl. Phys. Lett.* 47, 800-2.

Darken, L. S. (1948). xxx. *Trans. Met. Soc. AIME*, 175, 184-xxx.

Drehman, A. J., A. L. Greer, and D. Turnbull (1982). Bulk formation of a metallic glass: $Pd_{40}Ni_{40}P_{20}$. *Appl. Phys. Lett.* 41, 716-7.

Duwez, P., R. H. Willens, and W. Clement Jr. (1960. xxx. *J. Appl. Phys.* 31, 1136-xxx.

Greer, A. L. (1988). The thermodynamics of inverse melting. In Schwarz, R. B. and W. L. Johnson (eds.), *Solid State Amorphizing Transformations*, *J. Less-Common Met.* (in press).

Hahn, H, R. S. Averback, and H. -M. Shyu (1988). Diffusion studies in amorphous NiZr alloys and their relevance for solid state amorphizing reactions. In Schwarz, R. B. and W. L. Johnson (eds.), *Solid State Amorphizing Transformations, J. Less-Common Met.* (in press).

Hahn, H., R. S. Averback, and S. J. Rothman, (1986). Diffusivities of Ni, Zr, Au and Cu in amorphous Ni-Zr alloy. *Phys. Rev. B.* 33, 8825-8.

Hellstern, E and L. Schultz (1986). Glass forming ability in mechanically alloyed Fe-Zr. *Appl. Phys. Lett.* 49, 1163-5.

Hellstern, E., L. Schultz, and J. Eckert (1988). Glass-forming ranges of mechanically alloyed powders. In Schwarz, R. B. and W. L. Johnson (eds.), *Solid State Amorphizing Transformations, J. Less-Common Met.* (in press).

Johnson, W. L. (1986). Thermodynamic and kinetic aspects of the crystal to glass transformation in metallic materials. *Prog. in Mater. Science* 30, 81-134.

Kasiraj, P., T. Vreeland Jr., R. B. Schwarz, and T. J. Ahrens (1984). Shock consolidation of a rapidly solidified steel powder. *Acta Metall.* 32, 1235-41.

Kim, M. S. and C. C. Koch (19xx). Structural development during mechanical alloying of crystalline niobium and tin powders. *J. Appl. Phys.* xx, xxx-xx.

Kimura, H, M. Kimura, and F. Takada (1988). Development of extremely high energy ball mill for solid state amorphizing transformation. In Schwarz, R. B. and W. L. Johnson (eds.), *Solid State Amorphizing Transformations, J. Less-Common Met.* (in press).

Koch, C. C., O. B. cavin, C. G. McKamey, and J. O. Scarbrough (1983). Preparation of 'amorphous' $Ni_{60}Nb_{40}$ by mechanical alloying. *Appl. Phys. Lett.*, 43, 1017-1019.

Le Claire, A. D. (1978). Solute diffusion in dilute alloys. *J. Nuclear Mater.* 69 & 70, 70-96.

Lee, P. Y.,J. Jang, and C. C. Koch (1988). Amorphization by mechanical alloying: the role of mixtures of intermetallics. In Schwarz, R. B. and W. L. Johnson (eds.), *Solid State Amorphizing Transformations, J. Less-Common Met.* (in press).

Malik, S. K., and W. E. Wallace (1977). Hydrogen absorption and its effect on structure and magnetic behavior of $GdNi_2$. *Solid State Commun.* 24, 283-285.

Nash, P. and R. B. Schwarz (1988). Calculation of the glass forming range in binary metallic systems using thermodynamic models. *Acta Metall.*, submitted.

Niessen A. K., F. R. de Boer, R. Boom, P. F. de Châtel, W. C. M. Mattens, and A. R. Miedema (19xxx). *Model predictions for the enthalpy of formation of transition metal alloys II.* CALPHAD xxx, xxx-xxx.

Petrich, K. R. (1986). Synthesis and thermal properties of mechanically alloyed amorphous Ni-Ti powders. MS Dissertation, Illinois Int. of Tech., Chicago.

Rubin, J. and R. B. Schwarz (1988). Kinetics of the solid-state amorphizing reaction in thin films studied by electrical resistivity. *J. Appl. Phys.* (submitted).

Saunders, N. and A. P. Miodownik, (1986). Thermodynamic aspects of amorphous phase formation. *J. Mater. Res.* 1, 38-46.

Schlüter, H., H. C. Freyhardt, H. -U. Krebs, and R. Borman (1986). xxx. *Proc. 6th Int. Conf. on Liquid and Amorphous Met.*, Garmisch-Partenkirchen, xxxCity, pp xxx-xx.

Schultz L., and E. Hellstern (1987). Glass formation by mechanical alloying. *Mater. Res. Soc. Symp. Proc.* 80, 3-16.

Schultz, L. and E. Hellstern (1976). xxx. *Appl. Phys. Lett.* 48 (1976) 124-xx.

Schwarz, R. B. and W. L. Johnson (1983). Formation of and amorphous alloy

by solid-state reaction of pure polycrystalline metals. *Phys. Rev. Lett.* 51, 415-418.
Schwarz, R. B., R. R. Petrich, ans C. K. Saw (1985). The synthesis of amorphous Ni-Ti powders by mechanical alloying. *J. Non-Cryst. Solids* 76, 281-302.
Schwarz, R. B. and C. C. Koch (1985). Formation of amorphous alloys by the mechanical alloying of crystalline powders of pure metals and powders of intermetallics. *Appl. Phys Lett.* 49, 146-8.
Schwarz, R. B. (1986). Formation of amorphous metallic alloys by solid-state reactions. *Mater. Res. Bull.*, 11, 55-58.
Shingu, P. H. (1988). Metastability of amorphous phases and its application to the consolidation of rapidly quenched powder. *J. Mater. Sci. and Engineering*, in press.
Tiainen T. J. and R. B. Schwarz (1988). Synthesis and characterization of mechanically alloyed Ni-Sn powders. In Schwarz, R. B. and W. L. Johnson (eds.), *Solid State Amorphizing Transformations, J. Less-Common Met.* (in press).
Von Allmen, M. and A. Blatter (1987). Spontaneously vitrifying crystalline alloys. *Appl. Phys. Lett.* 50, 1873-75.
White, R. L. (1979). Ph.D. Dissertation, Stanford University.
Yeh, X. L., K. Samwer, and W. L. Johnson (1983). Formation of an amorphous metallic hydride by reaction of hydrogen with crystalline intermetallic compounds - A new method of synthesizing metallic glasses. *Appl. Phys. Lett.* 42, 242-44.
Yermakov, A. Ye., V. A. Barinov, and Ye. Ye. Yurchikov (1982). Variation of the magnetic properties of powders of Gd-Co alloys after refinement resulting in amorphism. *Phys. Met. Metall.* 54, 935-41.
Yermakov, A. Ye., Ye. Ye. Yurchikov, and V. A. Barinov (1981). Magnetic properties of amorphous powders of Y-Co alloys produced by grinding. *Phys. Met. Metall.* 52, 50-8.
Zöltzer K. and R. Bormann (1988). Thermodynamics of stable and metastable phases in the NiTi system and its application to amorphous phase formation. In Schwarz, R. B. and W. L. Johnson (eds.), *Solid State Amorphizing Transformations, J. Less-Common Met.* (in press).

FIGURE CAPTIONS

Fig. 1. Evolution of the solid-state amorphization reaction at the interfaces of a multilayer system of crystalline films of pure A and B (a), annealed at temperature T_r for time t_r (b). T_x is the crystallization temperature of the amorphous alloy. Th letters a, b, and c, correspond to those in Fig. 2.

Fig. 2. Resistance of a multilayer system of Ni and Zr thin films during the continuous heating and cooling at 10 K/min. The thermal cycle has been repeated twice. During the second cycle the resistance follows the line f-g traced during the cooling part of the first cycle. The letters a, b, and c correspond to those in Fig. 2.

Fig. 3. X-ray scattering intensity as a function of scattering angle for Au-La multilayers. Curves (*a*), (*b*), and (*c*) are for annealed samples with compositions Au-rich, equi-atomic, and La-rich, respectively. Curve (*d*) is for an unreacted (as deposited) multilayer with composition similar to that of curve (*b*).

Fig. 4. Schematic phase diagram (*a*) for a binary system, AB, with a

negative heat of mixing in the liquid state, and corresponding free-energy diagram at the temperature T_r (*b*). The bars at the bottom of the figure give the GFR predicted for the MA and the SSAR synthesis methods.

Fig. 5. Scanning electron micrograph of Ni and Ti powder after 0.5 h of MA.

Fig. 6. Scanning electron micrograph of the cross section of a flake-shaped particle shown in Fig. 5.

Fig. 7. Scanning electron micrograph of Ni and Ti powder after 25 h of MA.

Fig. 8. Scanning electron micrograph of the cross section of the amorphous particles shown in Fig. 7.

Fig. 9. X-ray diffraction intensity as a function of wavenumber *K* for a mixture of Ni and Ti powders mechanically alloyed for 2, 5, and 25 h.

Fig. 10. Comparison of the glass-forming ranges of rapidly solidified and mechanically alloyed Ni-Zr, Co-Zr, and Fe-Zr (from Hellstern, Schultz and Eckert, 1988).

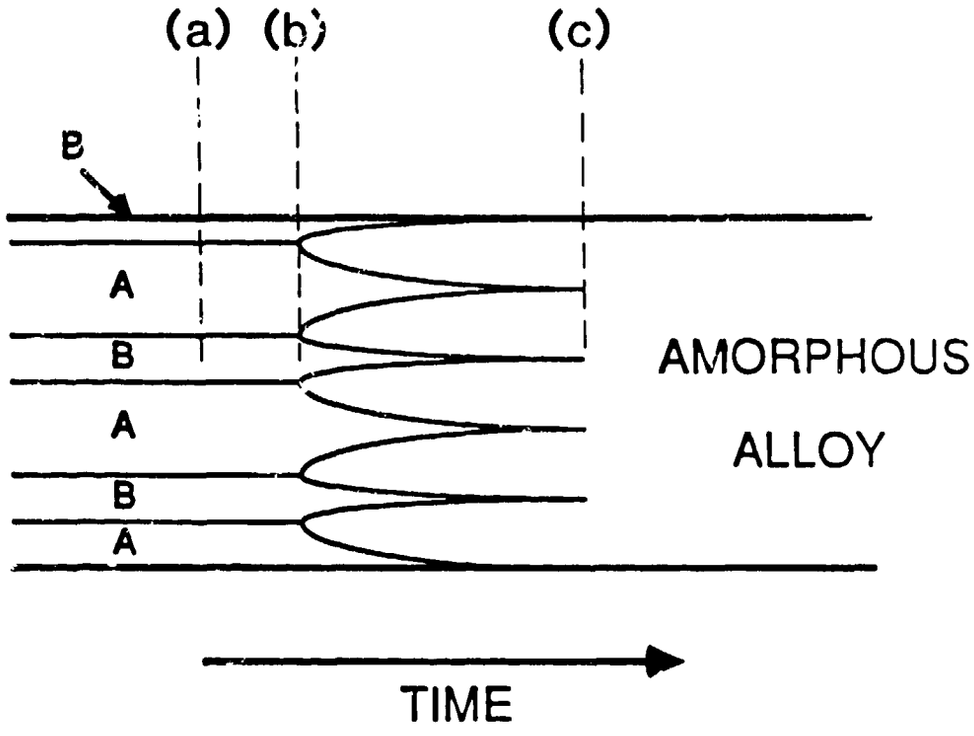

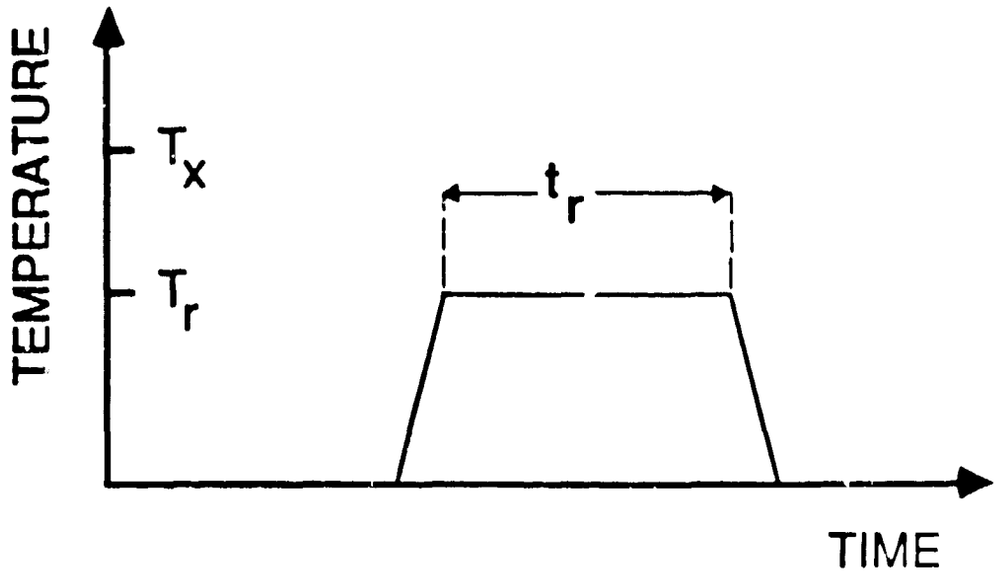

Fig.1

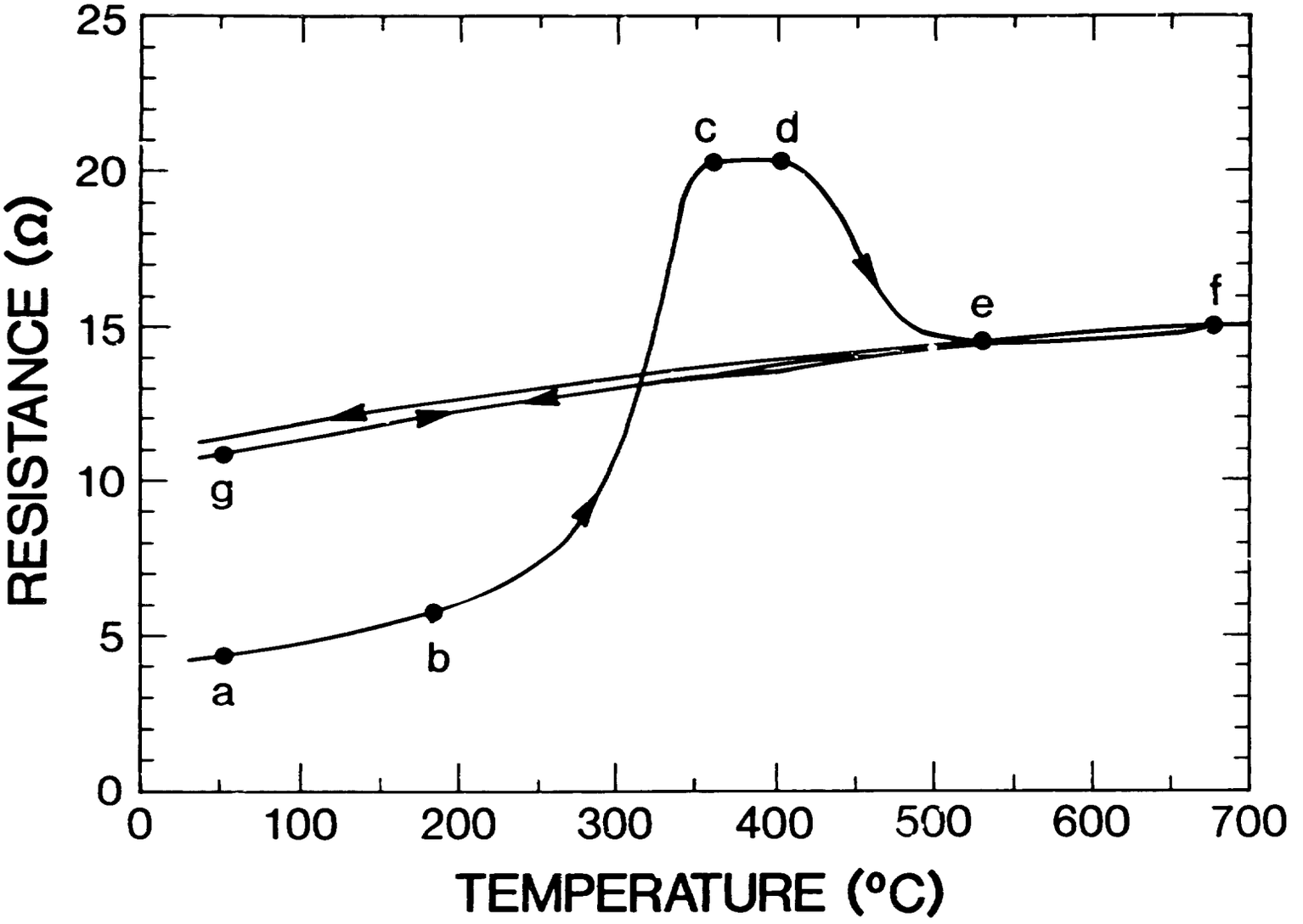
RESISTANCE (Ω)
TEMPERATURE (°C)
0
5
10
15
20
25
0
100
200
300
400
500
600
700
a
b
c
d
e
f
g

Fig. 2

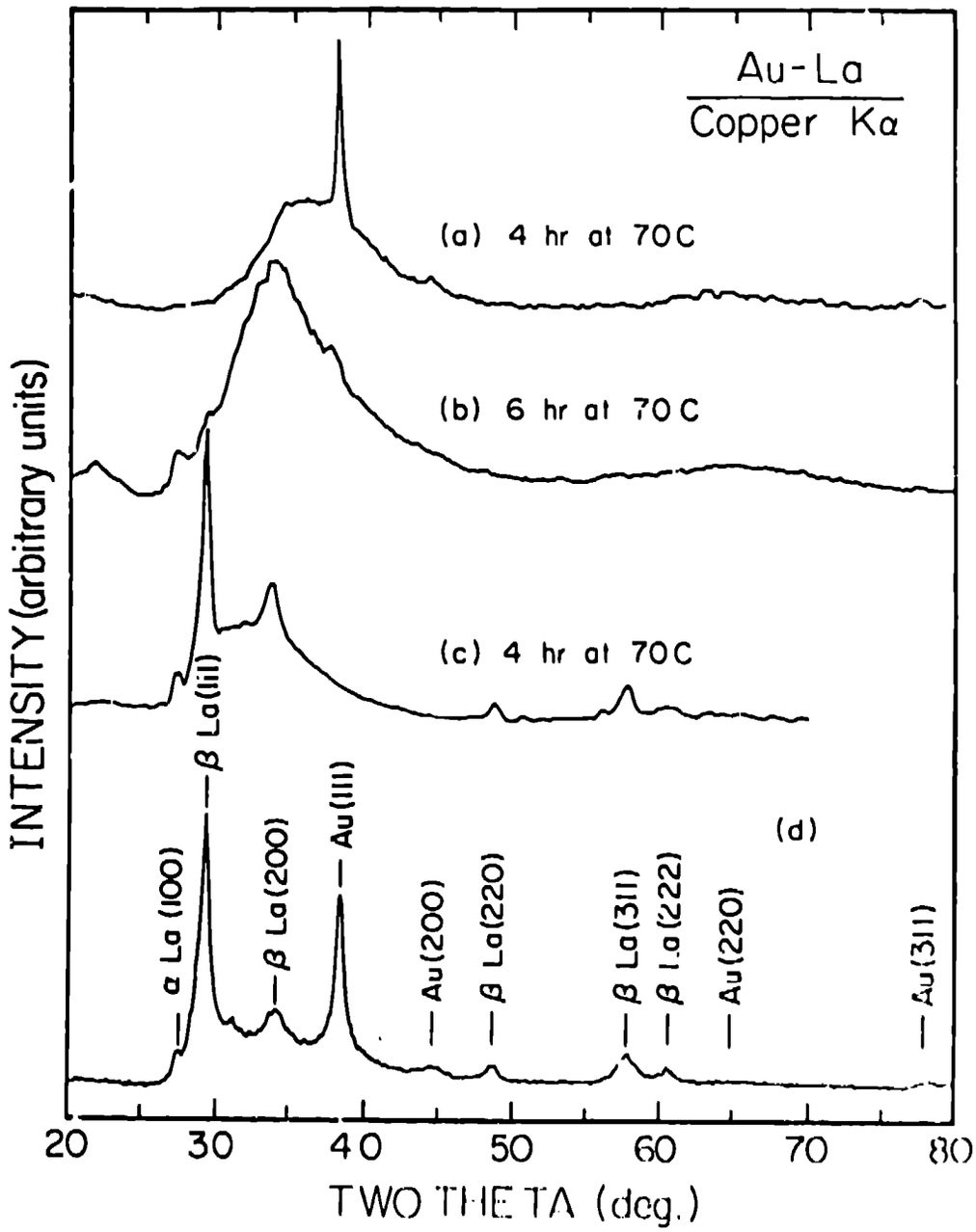
Au-La
Copper Kα
(a) 4 hr at 70C
(b) 6 hr at 70C
(c) 4 hr at 70C
(d)
α La (100)
β La(111)
β La(200)
Au(111)
Au(200)
β La(220)
β La(311)
β La(222)
Au(220)
Au(311)
INTENSITY (arbitrary units)
20
30
40
50
60
70
80
TWO THETA (deg.)

Fig. 3

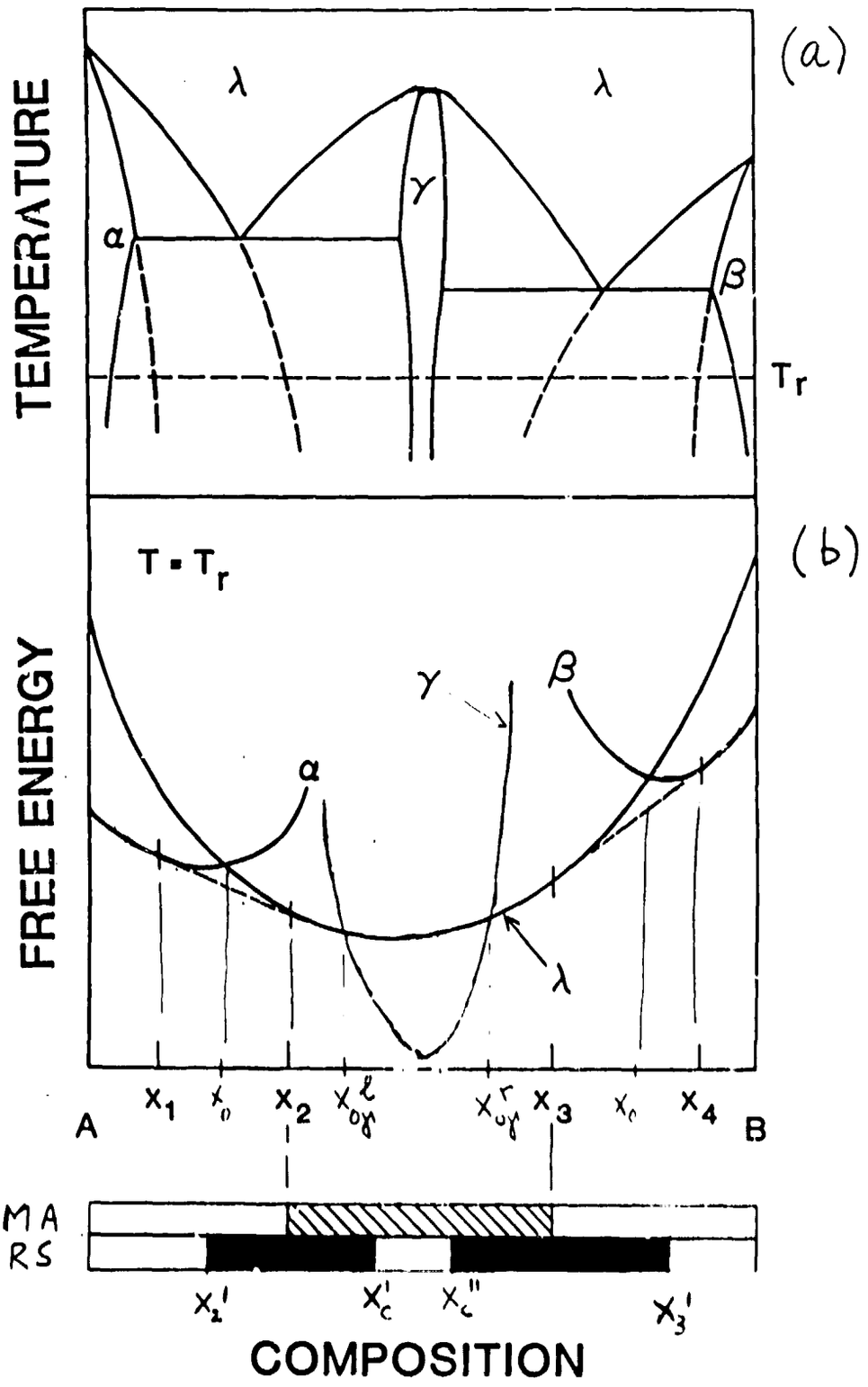
(a)
TEMPERATURE
λ
λ
γ
α
β
T_r
(b)
$T = T_r$
FREE ENERGY
γ
β
α
λ
x_1
x_0
x_2
$x_{0\gamma}^{\ell}$
$x_{0\gamma}^{r}$
x_3
x_0
x_4
A
B
MA
RS
x_2'
x_c'
x_c''
x_3'
COMPOSITION

Fig 4.

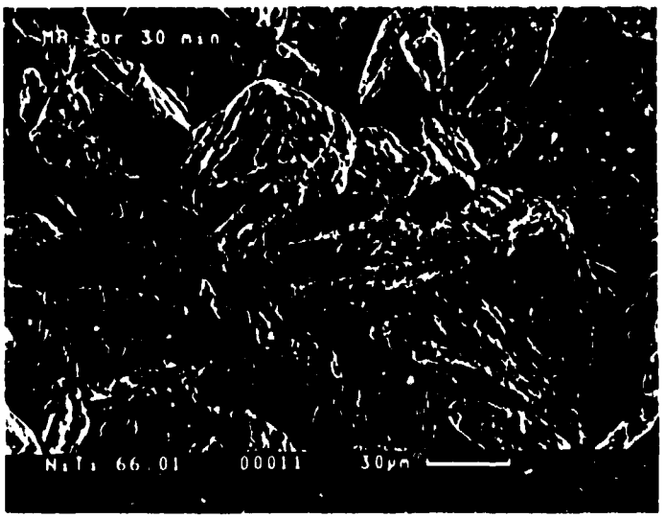

Fig. 5

Fig. 6

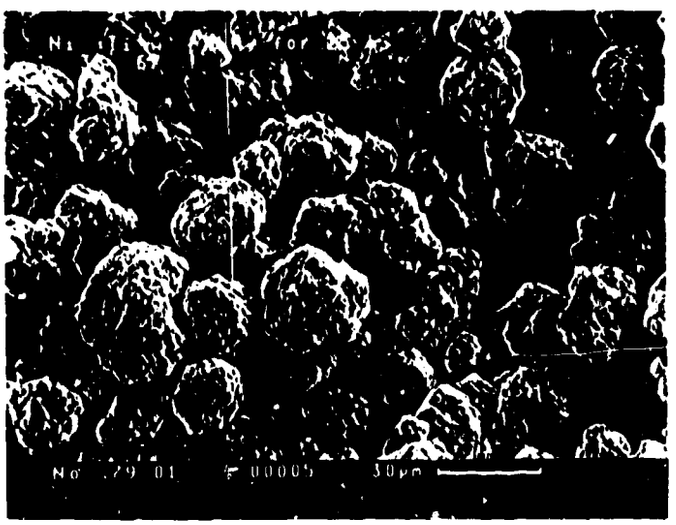

Fig. 7

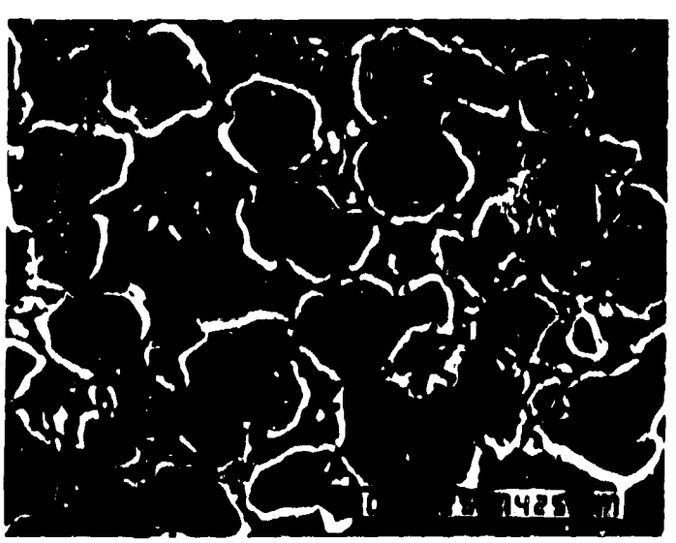

Fig 8

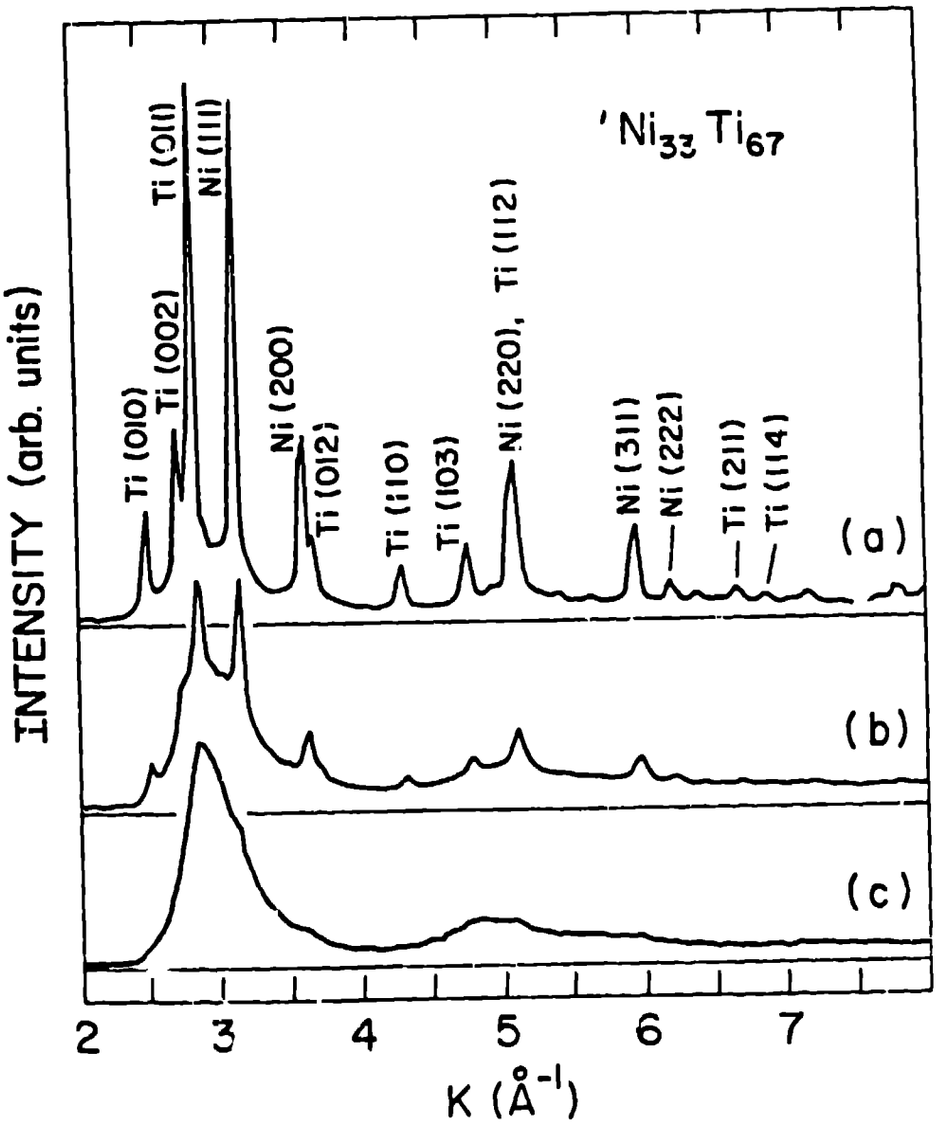
Ni33 Ti67
Ti (010)
Ti (002)
Ti (011)
Ni (111)
Ni (200)
Ti (012)
Ti (110)
Ti (103)
Ni (220), Ti (112)
Ni (311)
Ni (222)
Ti (211)
Ti (114)
(a)
(b)
(c)
INTENSITY (arb. units)
2
3
4
5
6
7
K (Å-1)

Fig. 9

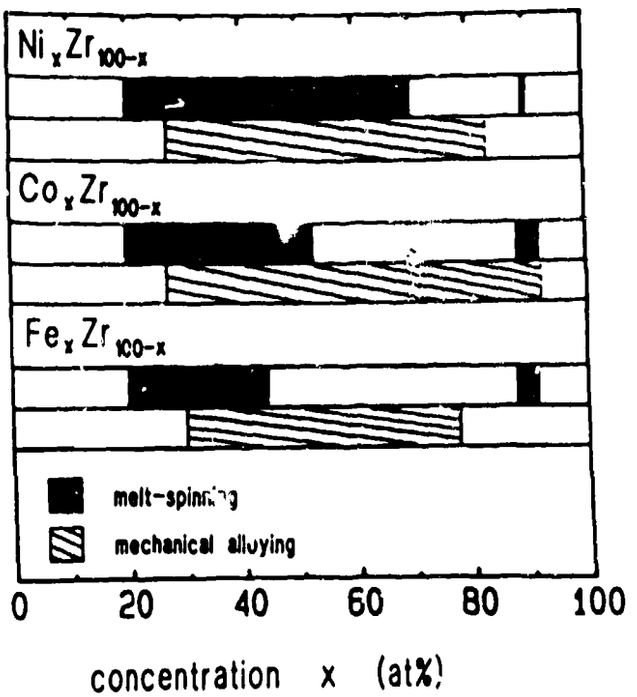
Ni_xZr_{100-x}
Co_xZr_{100-x}
Fe_xZr_{100-x}
melt-spinning
mechanical alloying
0
20
40
60
80
100
concentration x (at%)

Fig. 10